Int. J. Electrochem. Sci., 11 **(2016)** 8914 – 8926, doi: 10.20964/2016.11.06

International Journal of
ELECTROCHEMICAL
SCIENCE
www.electrochemsci.org

Short Communication

Enhanced Interphase Adhesion and Anticorrosion Properties in Epoxy Coating Modified via Acrylic Resin

Kai Wan [1,*], *Jiarun Li* [1,2], *Weichen Xu* [1], *Liangmin Yu* [3,*], *Baorong Hou* [1], *Min Liu* [4]

[1] Key Laboratory of Marine Environmental Corrosion and Bio-fouling, Institute of Oceanology, Chinese Academy of Sciences, Qingdao 266071, Shandong, China;
[2] University of Chinese Academy of Sciences, Beijing 100049, China
[3] Key Laboratory of Marine Chemistry Theory and Technology, Ministry of Education, Ocean University of China, Qingdao 266100, Shandong, China;
[4] Electric Power Research Institute, Zhejiang Power Corporation, State Grid Corporation of China, Hangzhou, 310000, Zhejiang, China
[*]E-mail: wank@qdio.ac.cn, yuyan@ouc.edu.cn

Received: 20 July 2016 / *Accepted:* 3 September 2016 / *Published:* 10 October 2016

Poly (α-methyl methacrylate-butyl acrylate-glycidyl methacrylate) (PMBG) and poly (α-methyl methacrylate-butyl acrylate) (PMB) were synthesized via solution polymerization and characterized via Fourier transform infrared spectroscopy (FTIR). And then, the modified epoxy coatings were prepared through dispersing 4 wt.% of PMBG and PMB in an epoxy coating through physical blending, respectively. The coatings were painted on the mild steel substrates and their anticorrosion performances were characterized by salt spray test and electrochemical impedance spectroscopy (EIS). Interphase adhesion was characterized by pull-off test. Incorporation of 4 wt.% of acrylic resin, especially PMB (as a constituent of the resin), into the epoxy coating significantly enhanced the anticorrosion performance and interphase adhesion of the coating (45%) through improving their inner structure.

Keywords: Organic coatings; Corrosion resistance; Interphase adhesion; Salt spray test; EIS

1. INTRODUCTION

Corrosion of metals has received a great deal of attention because of its economic and safety issues [1, 2]. Anticorrosion technology of metals usually includes the following methods such as electrochemical protection [3, 4], corrosion inhibitor [5, 6] and anticorrosion coatings [7]. One of the effective solutions is painting epoxy coating. Epoxy resin is considered as an applicable matrix that is widely used to protect steel reinforcements against corrosion under harsh environment [8, 9]. It has good mechanical performances, resistance to chemicals, electrical insulating properties, shielding

properties and strong cohesiveness to metal substrates. However, the epoxy coatings frequently suffer from aggressive environments such as ultraviolet light, salts, oxygen, water diffusion and so on, resulting in rapid deterioration [10].

Despite that epoxy coatings have desirable shielding properties and adhesion to substrates, water and oxygen are known to accumulate at the coating/metal substrate interface, where a series of chemical reactions can take place and corrosion products may be produced, resulting in a decrease of the bonding force which exists between substrate and coating, as well as between the layers of coatings [11, 12]. The adhesion between substrate and coating or interphase coating will suffer from weakening or breakage, leading to exfoliation of coating and corrosion of metal substrates. Therefore, the practical use of epoxy coatings in industry is limited.

In early studies, a lot of work on enhancing anticorrosion performance and adhesion has been reported [13-16]. In addition, J. van den Brand and his co-workers researched on improving the adhesion between the aluminum substrate and the epoxy coatings. They applied two different methods to improve the adhesion. The first method was by the application of thin functional polymeric layers, namely poly (acrylic acid) (PAA), poly (ethylene-alt-maleic anhydride) (PEMah) and poly (vinyl phosphonic acid) (PvPA) treatment on an aluminum substrate prior to painting the epoxy coating. The functional groups were capable to absorb on the oxide surface, and at the same time, they were also capable to take part in the chemical reactions with epoxy resin. The other method was by hydration of the aluminum substrates, performed by immersion in boiling water [17, 18]. Using silane coupling agents is also a way to improve the interphase adhesion. The silanes are applying to the metal surface performing metal-siloxane bonds and corresponding metal-siloxane interphase. This interphase is the link between coating and the substrate. The silane can be added to the resin, but without polymerization (curing), the silane interacts with metal performing chemical metal-siloxane bonds [19-25]. Dai and his co-works evaluated the adhesion between interfaces of a gelatin coating and poly (ethylene terephthalate) (PET) film using microscratch technique. The interface was reinforced by nitrogen plasma treatment on the PET surface and subsequently by heat treatment of each gelatin/PET sample to promote interactions at the interface [26]. Almost all the work has focused on improving the adhesion between substrate and coatings. To the best of my knowledge, there was a lack of knowledge on enhancing interphase adhesion because of a highly cross-linked structure of epoxy resin after curing. Hence, an approach in blending acrylic and epoxy resin physically has been proposed in the current work, in which the acrylic resin serves as a “micromolecule” compared to the epoxy resin, flowing into the epoxy systems to increase the coating density and then reduce the diffusion rate of oxygen and aggressive ions.

The evaluation methods of anticorrosion performance include conventional salt spray test and EIS measurements. EIS is important in monitoring and predicting degradation of organic coatings [27-30]. It has been utilized for evaluating steel bridge coating degradation because of its non-invasive nature and ability to detect subtle changes in coating properties. The use of EIS can obtain experimental data for characterizing organic coatings in corrosive environments which could not be obtained by means of salt spray test. For example, Hinderliter used EIS to develop a method to determine kinetic parameters and develop the theory of coating system [31][29]. Su studied on the deterioration process of bipolar coating using EIS [32].

In the current work, PMBG and PMB copolymer were synthesized via solution polymerization. The synthetic routes of PMBG and PMB were shown in Fig. 1. FTIR spectroscopy was used to determine the existence of epoxy group or whether the double bond was totally polymerized. The comparison methods of coatings on anticorrosion performance included salt spray tests and EIS measurements, and then pull-off test was used to obtain the value of interphase adhesion of epoxy coating. The microstructure of resins was analyzed by SEM.

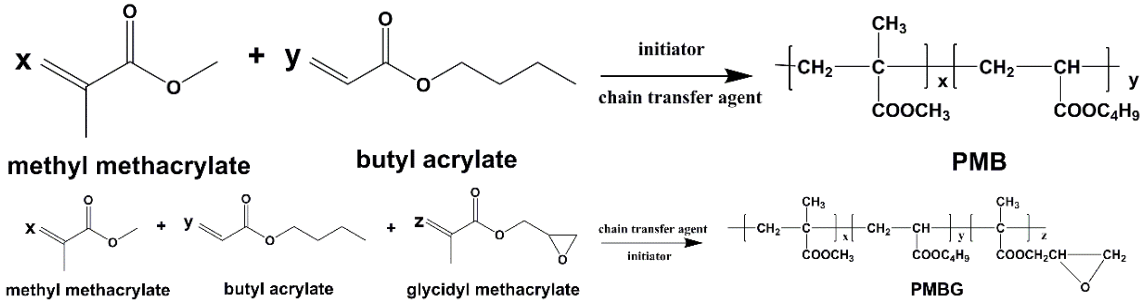

Figure 1. Synthetic routes of copolymers PMBG and PMB

2. EXPERIMENTAL

2.1. Materials and reagents

α-methyl methacrylate (MMA), butyl acrylate (BA) and glycidyl methacrylate (GMA) were purchased from Shanghai Aladdin Biochemical Technology CO., Ltd were distilled under reduced pressure. 2,2-azobisisobutyronitrile (AIBN) was provided by Beijing Chem. CO. DER331, a bisphenol-A liquid epoxy resin was applied by the Dow Chemical CO., Ltd. Polyamide curing agent2050 was obtained by the Air Products and Chemicals, Inc. Cold-roll steel sheets (150 mm × 75 mm × 1 mm, composition in wt.%: Fe: 97.5-97.8, C: 0.18-0.20, Si: 0.413-0.416, Mn: 1.38-1.40, P, S < 0.005, Cr: 0.024-0.027, Mo: 0.017-0.020, Co: 0.0557-0.0559, Cu: 0.0426-0.0430, Nb: 0.0480-0.0482) were polished using emery papers to a surface roughness of 3-5 μm and then degreased by acetone. The composition (in wt. %) of the Q235 steel electrode was C 0.18, Mn 0.51, Si 0.22, S≥ 0.05, P≥ 0.045.

2.2. Synthesis of MMA-BA-GMA and MMA-BA copolymers

PMBG and PMB copolymers were prepared by the solution polymerization reaction. The initiator was AIBN dissolved in the solvent butyl acetate (50 mL). MMA, BA and GMA were mixed, the remaining solvent was added to a 500 mL boiling flask-3-neck equipped with electric stirring, a water-cooled condensed a nitrogen inlet and outlet. The mixture was heated to 80° C, then the mixed monomer (20 mL) and the initiator (3 mL) were added to the solution to initiate the copolymerization. After heating for 15 min, the remaining monomer and initiator were divided to six copies and

respectively added to the solution every 15 min. After the copolymerization proceeded under continuous stirring for 3 h, the polymer solution was immediately poured out of the flask and kept in the dark. MMA / BA / GMA molar ratio of 6 / 3 / 1.5 was selected to prepare PMBG copolymers.

2.3. Sample preparation

The coating was a two-component cured epoxy resin with aluminum powder and a mixture of fillers. Synthetic acrylic resin was mixed into epoxy resin with a ratio of 10 wt.%, then the resin mixture with pigments and fillers except aluminum was dissolved in the right solvent (xylene/*n*-butanol, w/w = 7/3) and lapped for 45 min at a speed of 3500 r/min. Finally, the aluminum was added in the mixture and dispersed for 15 min at a speed of 1350 r/min. The polyamide curing agent and the resin were mixed and the mixture was painted onto steel panels with a soft brush. The coating thickness of dry film was 150-175 μm. After curing for 7 days, all the edges and backside of samples were sealed with a mixture of paraffin and colophony, leaving a central area unmasked. The salt spray test was accomplished through the standard ASTMD 1654-79.

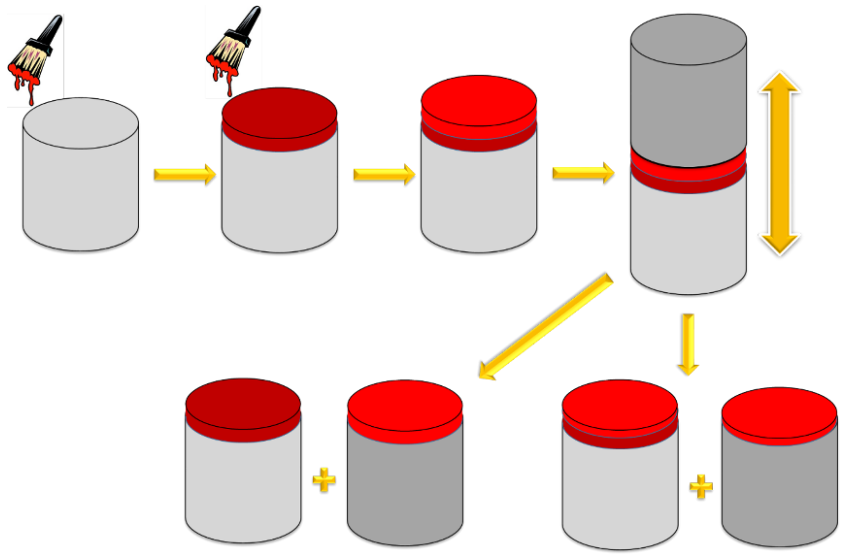

Figure 2. Schematic drawing of adhesion and cohesion failure of the coating after the pull-off adhesion test.

2.4. Characterization and testing

The structure of the copolymers was characterized by FTIR spectroscopy in order to certify if the double bond was totally polymerized and the epoxy group existed in the copolymer. The FTIR spectroscopy was recorded using an IFS-113 FTIR instrument. The morphology and structures of modified samples were observed by scanning electron microscope (SEM). Pull-off test of the coating was performed according to the national standard of China (GB/T 5210-2006: Paints and varnishes - pull-off test for adhesion), which was equal to the standard UNE-EN-ISO4624. The iron columns of 20

mm diameter were degreased in the acetone and then coated with two component coatings. After ten days curing, recoated the same coating for ten days curing as well. Finally, two components adhesive was glued to the surface of the cured coating. While the adhesive was cured, a testing equipment with loading fixture was strained at 3 mm/min in an AGS-J tensile machine until the coating stripping peeled from the coating. The diagram in preparation process of testing samples was shown in Fig. 2. The electrochemical impedance spectroscopy (EIS) tests of the coatings were performed on an AUTOLAB PGSTAT302N. All samples were immersed in natural seawater (NaCl 3.5 wt.%) open to the air at 25 ^{o}C before the electrochemical test [33]. EIS was performed with an 20 mV amplitude from the frequency $10^{5} \sim 10^{-2}$ Hz .

3. RESULTS AND DISCUSSION

3.1. FTIR analysis

The FTIR spectra of GMA monomer, PMBG and PMB are shown in Fig. 3. In the monomer and copolymers, the C-H stretching vibrations absorption bands around 2950 cm $^{-1}$ and 2850 cm $^{-1}$ are assigned to -CH_3 and the absorbance at 2930 cm $^{-1}$ is associated with - CH_2-. A strong absorption peak attributed to C=O ester carbonyl stretching vibration occurs around 1740 cm $^{-1}$. The C-H absorption peaks attributed to - CH_3 and - CH_2 appear at 1450 and 1387 cm $^{-1}$.

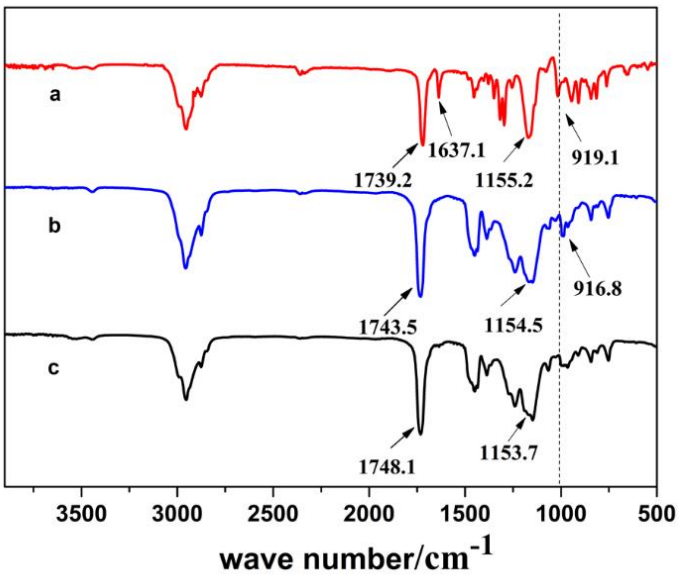

Figure 3. FTIR spectra of (a) GMA monomer (b) PMBG (c) PMB

A strong absorption band assigned to C-O-C stretching vibrations from ester groups occurs around 1150 cm $^{-1}$. The FTIR spectrum of the C-O-C stretching vibration absorption peaks 919.1 cm $^{-1}$ and 916.8 cm $^{-1}$ from epoxy group are attributed to GMA monomer and PMBG, respectively. Similar results are obtained in others' studies. For example, Luo et al [34]synthesized a novel copolymerarwith GMA and MMA, the C-O-C absorption peaks appear at 907 cm^{-1} and 1176 cm^{-1} belong to epoxy and

ester groups, respectively. Xia et al [35] also characterized the BA-MMA-GMA terpolymer using FTIR and drawn the same conclusion. In Hercigonja's study[36], the characterization results of copolymer proved our FTIR analysis. Moreover, there is no absorption peak of carbon-carbon double bond (1637.1 cm^{-1}) in both PMBG and PMB, indicating the complete polymerization of monomers and the existence of the epoxy group in PMBG.

3.2. Corrosion resistance performance of epoxy coating and modified epoxy coating

In order to evaluate the performance of the epoxy coating containing modified acrylic resin particle, three coated samples were prepared: (a) blank sample, (b) epoxy resin + PMBG, (c) epoxy resin + PMB. The photographs of the samples after 4000 h exposure in the salt spray chamber were presented in Fig. 4. The coating was intact outside the scratch without the presence of blister and rust [27]. It indicates that the coatings with good barrier property could effectively protect the substrate against corrosion. When the time of exposure to the salt spray increased, the edge of the rusty area spread out and the corrosion products sealed the scratch. After cleaning and peeling the coating, it was found that the sample c_2 showed the slightest rust-diffusion among the three samples. The highest corrosion resistance was shown on the epoxy coating treated by the PMB. When the corrosion resistance performance was evaluated through the diffusion of rust at the scratch on the substrate surface after the salt spray test. The anticorrosion efficiency of epoxy coating was rated as (c) > (b) > (a).

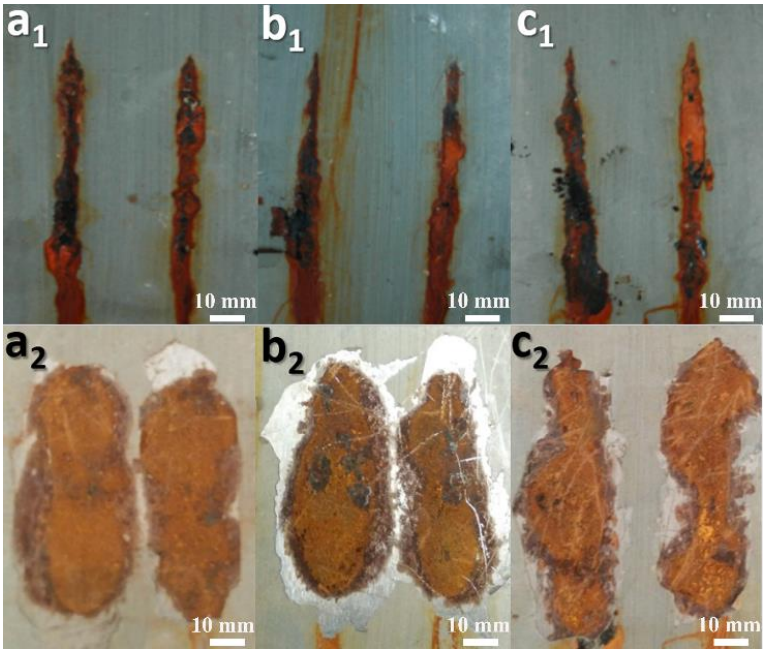

Figure 4. Photographs of the samples during 4000h exposition in the salt spray chamber. with scratch (a_1) blank sample (b_1) epoxy resin + PMBG (c_1) epoxy resin + PMB and stripping (a_2) blank sample (b_2) epoxy resin + PMBG (c_2) epoxy resin + PMB

3.3. EIS measurements and corrosion resistance mechanism

The EIS measurements were carried out to evaluate the corrosion resistance of epoxy coating. Fig. 5 showed the Nyquist (imaginary component of the impedance as a function of the real component) plots of carbon steel coated by modified epoxy coating in seawater as a function of different layers for immersion times, respectively. The electrochemical process was analyzed by the equivalent circuit method, and the corresponding physical model was presented in Fig.6. The Nyquist parameters obtained by using ZsimpWin impedance analysis software were presented in Table 1. In Fig. 6, R_s was solution resistance. C (Constant phase element — CPE) was employed with displacement of the "ideal" capacitance to describe non-uniform surface of the electrode. R_c represented coating resistance and C_c represented the respond of the double layer capacity of the solution/coating interface at high frequency. R_f represented the film resistance when electrolyte passed through the micropores of the coatings. R_{ct} was the charge transfer resistance, C_{dl} was corresponded to the capacitance and resistance of the electrode/coating interface in low frequency region. In addition, the capacitances were calculated using the equation developed by Hsu and Mansfield [37].

$$|Y|=Y_0\omega^n$$

Where the Y_0 (Ω^{-1} cm^{-2} s^{-1}) represented the frequency independent admittance of CPE, ω represented characteristic frequency, n (CPE exponent) was related to the angle of rotation of a purely capacitive line on the complex plane plots. n was generally close to 1 [38]. If n was equal to one, the CPE was equivalent to the pure capacitance, n was equal to 0.5, the CPE was equivalent to the Warburg impedance (Z_w) shown in Fig. 6c.

Fig. 5a showed no remarkable regularity of capacitance loops at the first 24 h immersion in the solution of three samples, Fig. 5b showed the Nyquist plots with the immersion time of 240 h. From the Figures, it could be seen that the impedance above the steel electrode decreased over the exposure time, dropping from 10^{10} Ω to 10^{8-9} Ω. Only one capacitance loop could be seen during these times and they showed the character of one time constant. However, for blank sample, a substantial decrease of capacitance loops occurred after the 720 h immersion, which meant the electrolyte solution had reached to the interface of coating/electrode. Corrosion electrochemistry reactions took place. At the immersion time of 2880 h, high frequency semicircle and low frequency diffusion arc occurred in the Nyquist plots, which was the indication of continual accumulation of corrosion products at electrode interface. For modified samples, it could be inferred from higher values of resistance parameters after 2880 hours of immersion, coatings formulated with modified epoxy resin provided more effective protection compared to the blank sample. The corrosion resistance efficiency was rated as epoxy resin + PMB > epoxy resin + PMBG > blank sample, the order of anticorrosion efficiency is consistent with the order of salt spray test as presented in Fig. 4 [39].

Results from the EIS test have been modelled with equivalent circuits shown in Fig. 6, and its characteristic parameters were determined. The fitting of the epoxy coating's spectra after immersion was carried out by employing the models above and the results are also shown in Fig. 6. The fitting results of experimental EIS data are presented in Table 1. Schematic diagram of electrochemical mechanism during the diffusion of electrolyte solution organic coating was generally considered as a kind of isolation layer. It protected the metal substrates from corrosion caused by infiltration of the

electrolyte onto substrate/coating interface. At the initial stage of immersion, diffusion of ions in electrolyte and oxygen seemed to occur in the coatings, indicating that barrier-type coating behavior could explain the impedance spectra (Fig. 7).

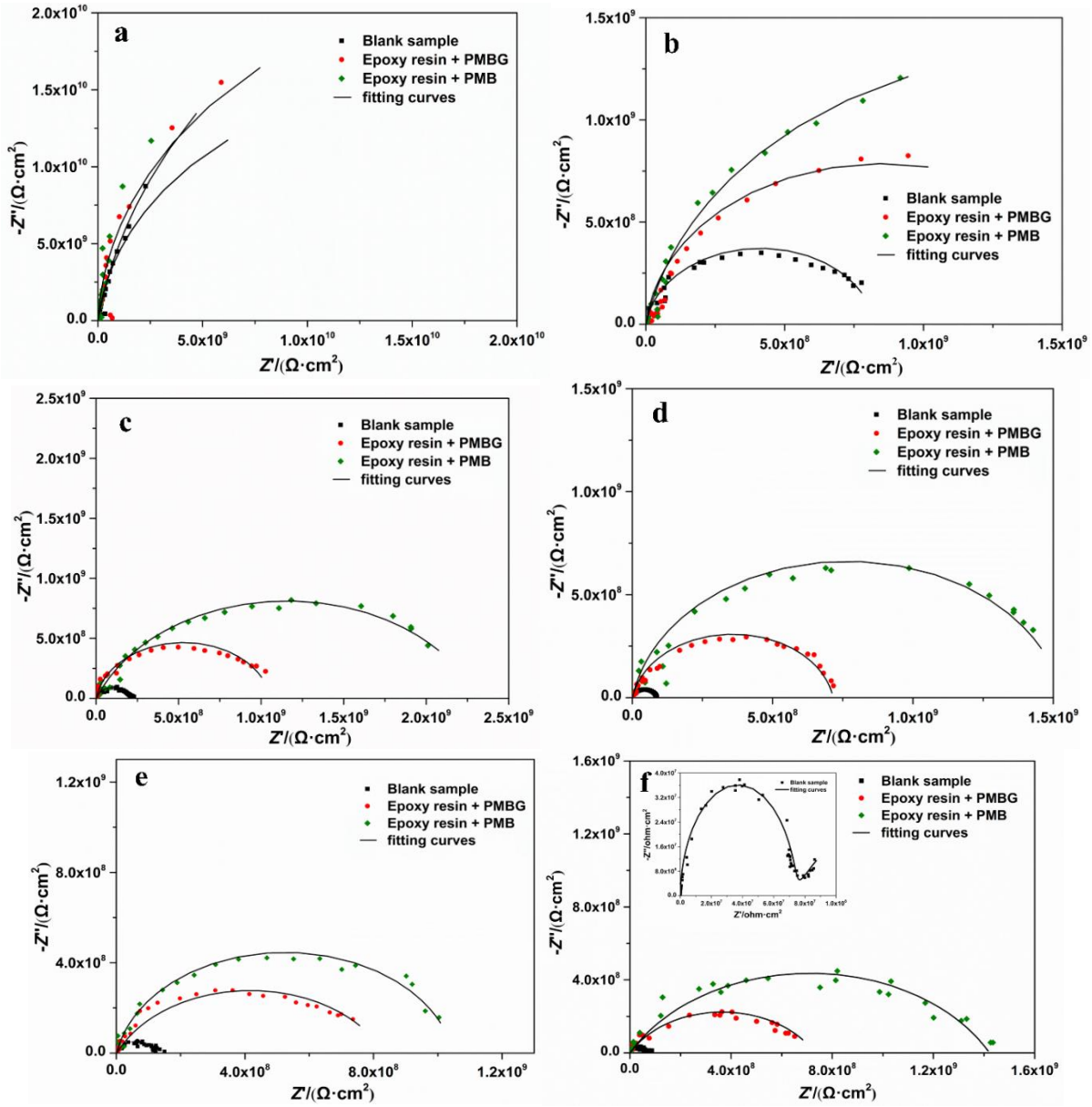

Figure 5. Nyquist plots of the EIS for a carbon steel coated with a 80 μm thick epoxy coating after immersion in sea water aqueous solution for different time. (a) 24 h (b) 240 h (c) 720 h (d) 1440 h (e) 1920 h (f) 2880 h.

Therefore, a capacitive behavior of the impedance, as deduced from the inspection of the spectra in Fig. 6 a was used. After infiltration of electrolyte into the coating and access the coating/substrate interface, the condition for electrochemical reactions on the metal surface would be established. The decrease in the coating resistance seemed to be a result of accommodation of ions from two sources, namely electrolyte and electrochemical reactions at the interface [40-42]. Hence, a

model of two constant (Fig. 6b) was used to interpret the mechanism mentioned above. The first time constant that appeared in the high frequency region was related to coating (a parallel circuit of coating capacitance C_c and film resistance R_f) and the second time constant which appeared in the low frequency corresponds to the coating/electrode interface (a parallel circuit of a C_{dl} and R_{ct} representing non-ideal double layer capacitance and charge transfer resistance, respectively). Notably, in the case of blank sample, a diffusion arc appeared owing to the faster infiltration speed through the coating. Some corrosion product generated on the coating/substrate interface, the R_f and R_{ct} values were much lower than the modified epoxy coatings. It was noted that the shielding performance of the pure epoxy coating was worse than modified coatings. Furthermore, owing to particles blocking effect, the electrolyte permeated deviously into the coating to the coating/substrate, namely "tangential diffusion" [43]. Therefore, an equivalent circuit model was used to interpret the corrosion mechanism of the blank sample (Fig. 6c).

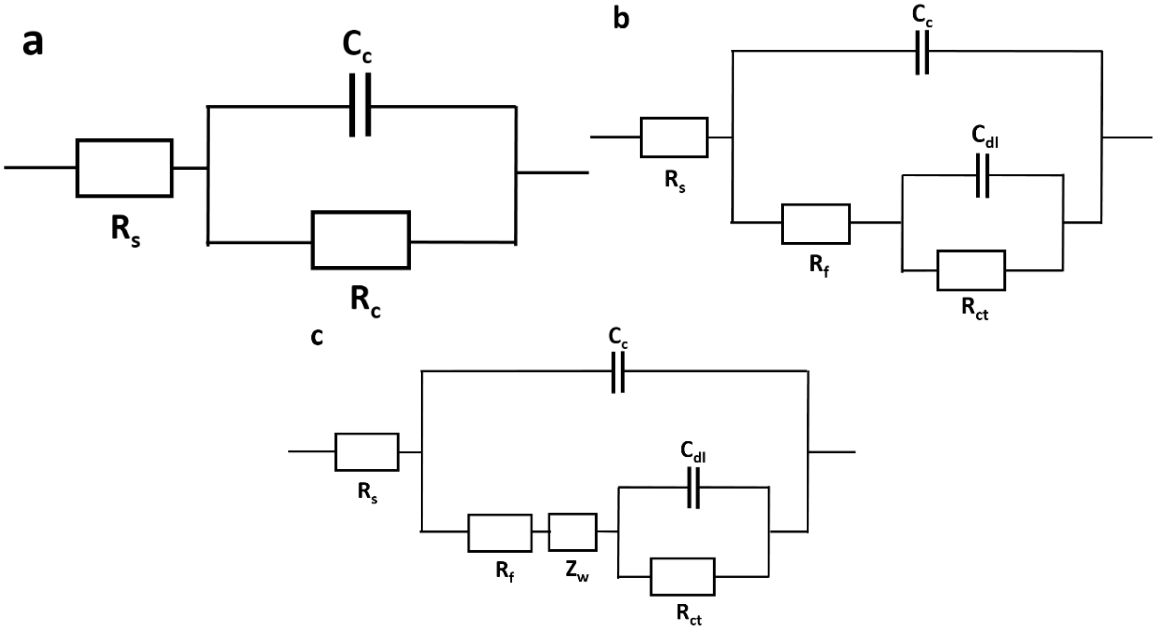

Figure 6. Equivalent circuit model for impedance plots of carbon steel coated with epoxy coating in seawater aqueous solution. (a) immersing for 24 h of three samples (b) immersing for 2880 h of samples Epoxy resin + PMBG and Epoxy resin + PMB (c) immersing for 2880 h of blank sample.

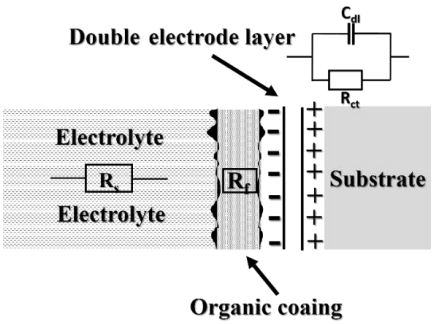

Figure 7. Schematic diagram of electrochemical mechanism during the diffusion of electrolyte solution

Table 1. Impedance data for carbon steel coated with epoxy coating in seawater with different immersion times

Samples (24 h)	$R_c/\Omega \cdot cm^2$	$Y_0/(\Omega^{-1}\ cm^{-2}\ s^{-1})$	n
Blank sample	2.6×10^{10}	3.4×10^{-7}	0.95
Epoxy resin + PMBG	6.6×10^{10}	2.3×10^{-10}	0.95
Epoxy resin + PMB	8.9×10^{10}	2.4×10^{-10}	0.91

Samples (2880 h)	R_s ($\Omega\ cm^2$)	Y_0 ($\Omega^{-1}\ cm^{-2}\ s^{-1}$)	n	R_f ($\Omega\ cm^2$)	Y_0' ($\Omega^{-1}\ cm^{-2}\ s^{-1}$)	n	R_{ct} ($\Omega\ cm^2$)	Z_W ($\Omega^{-1}\ cm^{-2}\ s^n$)
Blank sample	100	3.1×10^{-10}	0.98	1.8×10^{8}	7.2×10^{-10}	0.87	1.2×10^{8}	1.2×10^{-10}
Epoxy resin + PMBG	90	2.8×10^{-10}	0.94	6.8×10^{8}	5.4×10^{-10}	0.89	2.8×10^{8}	-
Epoxy resin + PMB	80	1.4×10^{-10}	0.97	1.3×10^{9}	5.4×10^{-10}	0.91	6.0×10^{8}	-

3.4. Pull-off tests and morphology observation

To test the adhesion strength of the epoxy coating for the different systems, pull-off tests were carried out. Each sample was tested six times and the average value was taken [44, 45]. Fig. 8 showed the adhesion strength needed to pull apart two pieces of coated steel glued together by the tensile machine in the adhesion test. The test results of numerical precision were estimated to be 1 MPa. In the case of blank sample, a value of 9 MPa was measured, which was slightly lower than the coating treated with PMBG. However, in the case of the coating treated with PMB, the pull-off strength value was 13 MPa [16], with an improvement of 45%. The consequence indicated that interphase adhesion of the epoxy coating with PMB would be effectively improved. A better adhesion was benefited from the change of microstructure shown in Fig. 8. It was observed in Fig. 9a that some corrugation like ravines existed in the cross-section morphological structure of pure epoxy resin. From Fig. 9d, messy inner row w seen in the longitudinal section of the sample. When a same coating was painted again on a fully cured coating, large quantities of vapor and air were filled into the interphase, resulting in the decrease of the adhesion and barrier performance. When PMBG was added into the epoxy coating, the acrylic resin might flow into the spare space of cured epoxy structure. At the same time, PMBG could react with curing agent due to the epoxy group, showing both the property of epoxy resin and acrylic resin. However, the detects of morphological structure could not be remedied completely (Fig. 9b). The addition of PMB into epoxy coating made morphological structure more compact and smoother than the other two samples because of its good flowability (Figs. 9c and 9f). The corrosion resistance maintained and interphase adhesion was promoted, which was consistent with the results of salt spray tests and EIS measurements.

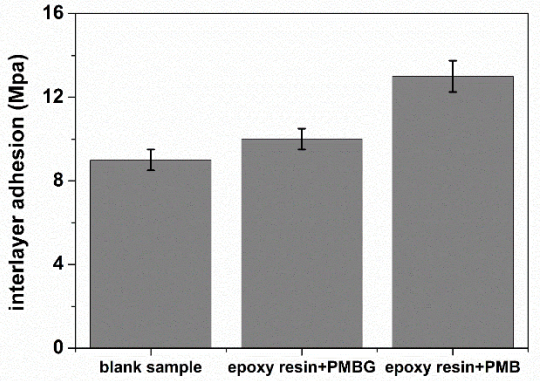

Figure 8. Pull-off adhesion strength of three samples

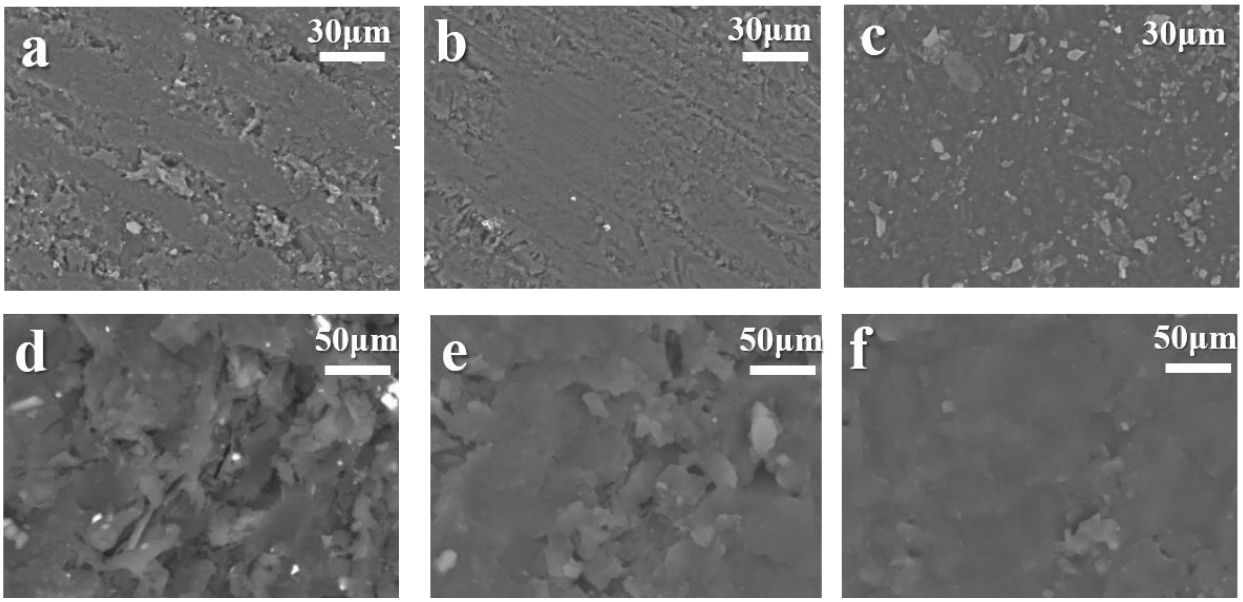

Figure 9. SEM photographs of resins without pigments and fillers (a) ~ (c) for cross-section, (d) ~ (f) for longitudinal section, (a) and (d) Blank sample, (b) and (e) epoxy resin + PMBG, (c) and (f) epoxy resin + PMB

4. CONCLUSIONS

The corrosion resistance and interphase adhesion of modified epoxy coatings have been studied, and several conclusions were drawn as follows:

(1) Acrylic resins PMBG and PMB were successfully synthesized via solution polymerization, which was proved by the FIRT results.

(2) The results of both 4000 h salt spray tests and EIS measurements after 2880 h immersion indicated that the corrosion resistance was promoted for the modified coatings, and the coating treated by PMB was the optimal.

(3) Pull-off strength tests and SEM observations showed that the interphase adhesion of epoxy coatings was improved via modification with PMBG and PMB. The adhesion strength value of the epoxy coating with PMB was increased by 45% compared to the pure epoxy coating attributed to the more compact internal structure.

ACKNOWLEDGEMENTS
The authors gratefully acknowledge financial support by National Natural Science Foundation of China (Nos. 51003099 and 51102219), the National Key Technology Research and Development Program of the Ministry of Science, Technology of China (No.2012BAB15B02) and Postdoctoral Science Foundation of Qingdao and Program of State Grid Corporation of Science and Technology.

References

1. K.N. Allahar, M.E. Orazem, *Corros. Sci.*, 51 (2009) 962-970.
2. N. Ahmad, A.G. MacDiarmid, *Synth. Met.*, 78 (1996) 103-110.
3. G. Grundmeier, W. Schmidt, M. Stratmann, *Electrochim. Acta*, 45 (2000) 2515-2533.
4. T. Shimura, K. Aramaki, *Corros. Sci.*, 50 (2008) 292-300.
5. M. Saremi, M. Yeganeh, *Corros. Sci.*, 86 (2014) 159-170.
6. S.-H. Yoo, Y.-W. Kim, K. Chung, N.-K. Kim, J.-S. Kim, *Ind. Eng. Chem. Res.*, 52 (2013) 10880-10889.
7. A. Ghanbari, M. Attar, M. Mahdavian, *Mat. Chem. Phy.*, 124 (2010) 1205-1209.
8. Y. Zuo, L. Zhang, X. Zhao, Y. Tang, X. Zhang, *J. App. Polym. Sci.*, 132 (2015) 46989.
9. M. Conradi, A. Kocijan, M. Zorko, I. Verpoest, *Prog. Org. Coat.*, 80 (2015) 20-26.
10. X. Li, X. Nie, L. Wang, D. Northwood, *Surf. Coat. Tech.*, 200 (2005) 1994-2000.
11. T. Nguyen, E. Byrd, D. Bentz, *J. Adhes.*, 48 (1995) 169-194.
12. T. Nguyen, E. Byrd, D. Bentz, C. Lint, *Prog. Org. Coat.*, 27 (1996) 181-193.
13. A. Kinloch, *Adhes. Adhes.*, Chapan and Hall, (1987).
14. A.A. Roche, J. Bouchet, S. Bentadjine, *Int. J. Adhes. adhes.*, 22 (2002) 431-441.
15. K.L. Mittal, *Springer*, 1 (1983) 589-668.
16. C.-W. Chang, K.-T. Lu, *J. App. Polym. Sci*, 115 (2010) 2197-2202.
17. J. Van den Brand, S. Van Gils, H. Terryn, V. Sivel, J. de Wit, *Prog. Org. Coat.*, 51 (2004) 351-364.
18. J. Van den Brand, S. Van Gils, P. Beentjes, H. Terryn, V. Sivel, J. De Wit, *Prog. Org. Coat.*, 51 (2004) 339-350.
19. N.L. Thomas, *Prog. Org. Coat.*, 19 (1991) 101-121.
20. G. Walter, *Corro. Sci.*, 26 (1986) 27-38.
21. B. Ramezanzadeh, S. Niroumandrad, A. Ahmadi, M. Mahdavian, M.H.M. *Corros. Sci.*,103 (2016) 283-304.
22. V. Arslanov, *J. Adhes.*, 44 (1994) 257-269.
23. N. Rezaee, M. Attar, B. Ramezanzadeh, *Surf. Coat. Tech.*, 236 (2013) 361-367.
24. H. Leidheiser, W. Funke, *J. Oil Col. Chem. Asso.*, 70 (1987) 121-132.
25. W. Funke, *J. Oil Col. Chem. Asso.*, 68 (1985) 229-232.
26. C.-A. Dai, C.-C. Liao, T.-A. Tsui, H.-C. Chien, M.-W. Liu, *J. App. Polym. Sci.*, 99 (2006) 1960-1974.
27. Y. Shao, C. Jia, G. Meng, T. Zhang, F. Wang, *Corros. Sci.*, 51 (2009) 371-379.
28. G. Walter, *Corro. Sci.*, 32 (1991) 1353-1376.
29. Y. Huang, H. Shih, H. Huang, J. Daugherty, S. Wu, S. Ramanathan, C. Chang, F. Mansfeld, *Corro. Sci.*, 50 (2008) 3569-3575.
30. M. Behzadnasab, S. Mirabedini, K. Kabiri, S. Jamali, *Corros. Sci.*, 53 (2011) 89-98.

31. B. Hinderliter, *ECS Transactions*, 41 (2012) 39-51.
32. X. Su, Q. Zhou, Q. Zhang, Y. Zhang, H. Zhang, *App. Surf. Sci.*, 257 (2011) 6095-6101.
33. G. Gupta, N. Birbilis, A. Khanna, An Epoxy Based Lignosulphonate Doped Polyaniline-Poly (Acrylamide Co-Acrylic Acid) Coating for Corrosion Protection of Aluminium Alloy 2024-T3, *Int. J. Electrochem. Sci,* 8 (2013) 3132-3149.
34. D. Luo, P. Li, M. Yang, *J. App. Polym. Sci.,* 118 (2010) 1527-1533.
35. R. Xia, M. Li, Y. Zhang, J. Qian, X. Yuan, *J. App. Polym. Sci.,* 119 (2011) 282-289.
36. R. Hercigonja, D. Maksin, A. Nastasovic, S. Trifunovic, P. Glodic, A. Onjia, *J. App. Polym. Sci.,* 123 (2012) 1273-1282.
37. C. Hsu, F. Mansfeld, *Corrsos.* , 57 (2001) 747-748.
38. J.-B. Jorcin, E. Aragon, C. Merlatti, N. *Corro. Sci.*, 48 (2006) 1779-1790.
39. J.H. Park, T.H. Yun, K.Y. Kim, Y.K. Song, J.M. Park, *Prog. Org.Coat.*, 74 (2012) 25-35.
40. R. Naderi, M. Attar, *Corros. Sci.*, 52 (2010) 1291-1296.
41. A. Mostafaei, F. Nasirpouri, *Prog. Org.Coat.*, 77 (2014) 146-159.
42. X. Yuan, Z.F. Yue, X. Chen, S.F. Wen, L. Li, T. Feng, *Prog. Org.Coat.*, 86 (2015) 41-48.
43. C.L. Zeng, W. Wang, W.T. Wu, *Corro. Sci.*, 43 (2001) 787-801.
44. R. Mafi, S.M. Mirabedini, R. Naderi, M.M. Attar, *Corros. Sci.*, 50 (2008) 3280-3286.
45. M. Niknahad, S. Moradian, S.M. Mirabedini, *Corros. Sci.*, 52 (2010) 1948-1957.